



Fruit cracking in muskmelon: Fruit growth and biomechanical properties in different irrigation levels

Qimin Xue^{a,b,c}, Hao Li^{a,b,c}, Jinliang Chen^{a,b,c}, Taisheng Du^{a,b,c,*}

^a State Key Laboratory of Efficient Utilization of Agricultural Water Resources, Beijing 100083, China

^b National Field Scientific Observation and Research Station on Efficient Water Use of Oasis Agriculture in Wuwei of Gansu Province, Wuwei, Gansu province 733009, China

^c Center for Agricultural Water Research in China, China Agricultural University, Beijing 100083, China

ARTICLE INFO

Handling Editor: Dr Z Xiyang

Keywords:

Fruit cracking
Fruit growth
Cuticle
Biomechanics
Irrigation

ABSTRACT

Muskmelon cracking during ripening is a physiological disorder that causes severe economic losses. Cracking is related with fruit growth, cuticular membrane (CM), biomechanics and cell wall. Nevertheless, the mechanism of cracking induced by irrigation strategy remains unclear. Therefore, we conducted an experiment in muskmelon grown under three irrigation levels: full irrigation (T1, 100% ET), mild deficit irrigation (T2, 75% ET of T1), and severe deficit irrigation (T3, 50% ET of T1). The results showed that fruit mass of T2 and T3 at maturity were decreased by 11.06% and 19.67%, while fruit cracking rate decreased by 53.13% and 84.38% compared to T1, respectively. Irrigation modified fruit growth rate during fruit expanding (Stage I) and maturation stage (Stage II), with a higher growing rate observed under high irrigation levels. Furthermore, fruits under T2 and T3 had a significantly less deformable (lower strain rate) cuticle than that under T1, resulting in higher CM per unit fruit surface area. The mechanical properties showed different dynamic mode during fruit growth. The pericarp break force and pericarp toughness increased at Stage I and then decreased at Stage II, while pericarp brittleness displayed an increasing trend before harvest. We concluded that deficit irrigation alleviated the fruit cracking by adjusting fruit growth rate, and increasing the pericarp break force and toughness at Stage II. However, both of T1 and T3 resulted in accelerated cell wall decomposition during fruit ripening. Therefore, mild deficit irrigation is an appropriate practice strategy that can greatly mitigate fruit cracking while slightly reducing fruit growth.

1. Introduction

Fruit cracking, as a serious physiological disorder commonly found in several fruit species, can cause huge economic losses. The water inflow from the plant to the fruit increases the cell turgor pressure within fruit, causing tangential skin strain (Grimm et al., 2019). Crack occurs when internal pressure exceeds the breaking stress of the epidermis (Brown and Considine, 1982). Many factors are involved in fruit cracking, such as environmental conditions, cultivation practices and fruit biochemical properties, all of which are all linked to fruit water balance (Saei et al., 2014; Wang et al., 2021). As one of the most important cultivation practices, irrigation greatly affect the yield and quality of crops (Sensoy et al., 2007). Deficit irrigation (DI) is an effective strategy that attempts to improve water use efficiency and fruit quality without compromising fruit yield by appropriately reducing water supply (Du et al., 2015; Hou et al., 2020). Furthermore, many

studies have shown that an appropriate irrigation management can also effectively reduce the probability of fruit cracking in tomato (Peet and Willits, 1995), apple (Opara et al., 2000), fig (Kong et al., 2013), sweet cherry (Blanco et al., 2019), and jujube (Wang et al., 2021). However, there is little in-depth research on the impact of deficit irrigation on fruit cracking.

The cuticle (syn. cuticular membrane CM) is a lipoidal, extracellular biopolymer that forms the outermost layer of the epidermis, serving as the primary barrier to water transport (absorption and loss) and a protective barrier to attack by insects and diseases (Domínguez et al., 2011). The cuticle is considerably vital for the structural integrity and, as such, plays a prominent role in fruit cracking. The fruit cracking is mostly derived from the formation of microcracks in the cuticular membrane (CM) serving as focal points weakening the dermal system (Brown and Considine, 1982). Generally, the cracks in the CM result from marked elastic strain of the CM, due to that fruit CM deposition does not keep

* Correspondence to: Center for Agricultural Water Research in China, China Agricultural University, 15, Beijing 100083, China.

E-mail address: dutaisheng@cau.edu.cn (T. Du).

<https://doi.org/10.1016/j.agwat.2024.108672>

Received 9 October 2023; Received in revised form 21 December 2023; Accepted 2 January 2024

Available online 23 January 2024

0378-3774/© 2024 The Authors. Published by Elsevier B.V. This is an open access article under the CC BY-NC license (<http://creativecommons.org/licenses/by-nc/4.0/>).

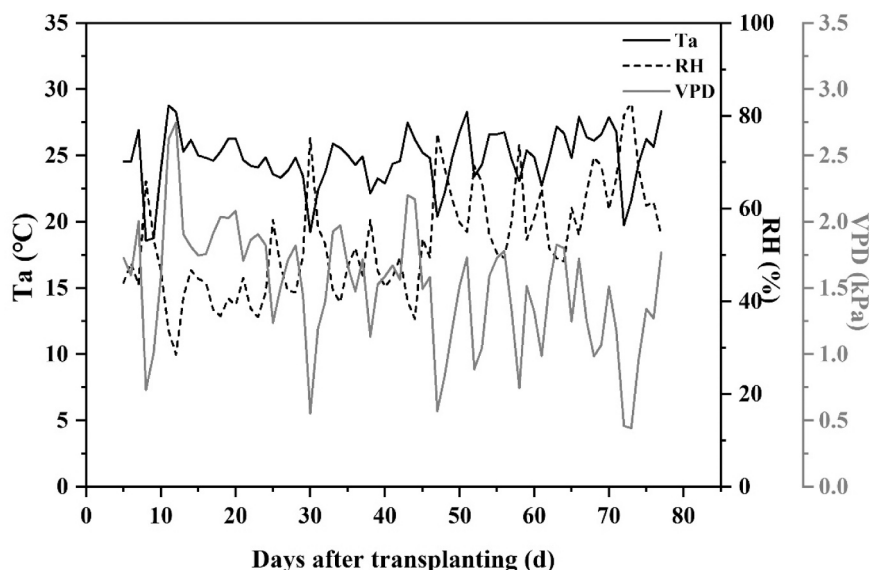


Fig. 1. Daily changes of air temperature (Ta), relative humidity (RH), vapor pressure difference (VPD) in the greenhouse during the whole growth period of muskmelon.

pace with the rapid expansion of fruit surface area (Knoche et al., 2004). Additionally, owing to the sudden and drastic change in stress-bearing properties during fruit-ripening process, the outer cuticle has to bear more tensional forces transmitted from the soft flesh cells (Chang et al., 2019). Many studies reported that the strain of the CM was closely related to fruit surface expansion and CM deposition in sweet cherry (Knoche et al., 2004), jostaberry (Khanal et al., 2011), and apple (Lai et al., 2016). However, few studies have been down on the effect of irrigation on CM stain and synthesis.

The biomechanical properties of fruit play a significant role in sustaining inner pressure and resistance to fruit cracking (Saei et al., 2014). Specially, the knowledge of the mechanical properties of pericarp is of vital interest, and several studies have been carried out in tomato (Bargel and Neinhuis, 2005; Domínguez et al., 2012), apple (Winisdorffer et al., 2015), and jujube (Li et al., 2018). The fruit crack resistance is highly related to pericarp toughness and extensibility (Li et al., 2018). Fruit cracking is positively correlated with rind hardness, and negatively correlated with pericarp break forces (Yamaguchi et al., 2002; Liao et al., 2020). It has also been reported that immature fruits have a higher degree of elasticity than mature ones, but fruit cracking mostly occurs during the mature stage (Li et al., 2021a). The structure and composition of the cell wall directly determine fruit mechanical properties, hence, the fruit strength (Cybulska et al., 2011). The polysaccharide network structure of cell wall is composed of cellulose, hemicellulose, and protopectin. Protopectin contains an interlamellar bond between adjacent cells, which tightly binds plant tissue cells through cross-linking of different polymers and proteins in cell walls (Verbančić et al., 2018). And the percentage of the water-soluble pectin (WSP) increases towards maturity, due to the dissolution of pectin (Ponce et al., 2010; Rolle et al., 2012). Cellulose is the main component of plant cell wall, and plays a crucial role in the bearing strength of cell wall. Hemicellulose is considered as the main polymer, which connects cellulose microfibrils in different areas of the cell wall and forms a cellulose-hemicellulose network (Deng et al., 2013). Some studies have shown that cellulose and hemicellulose decomposition, and the increase of WSP might lead to the cracking of fruit during ripening and a shorter shelf-life (Wang et al., 2023). The degradation of the structural components necessary to reinforce the cell wall is a characteristic of the fruit-ripening process (Brüeggewirth and Knoche, 2017), which is associated with a rapid decline in splitting resistance (Domínguez et al., 2012; Chang et al., 2019). Biomechanical properties of pericarp and cell

wall structure play an important role in fruit cracking, because both of them are linked to internal pressure resistance (Lichter et al., 2002). Therefore, it is essential to understand the response of biomechanical properties of fruit peel and cell wall components during fruit development and maturation to different water supplement.

Melon (*Cucumis melo L.*) is a worldwide horticultural crop with high nutritional characteristics and market value (Yavuz et al., 2021). The melon is likely to splitting and cracking at maturity stage, causing a serious detrimental effect on its market acceptability and economic benefit (Lopez-Zaplana et al., 2022). It has been reported that melon cracking is related to rapid water absorption, which can induce high cell turgor pressures, leading to pericarp cracking (Lopez-Zaplana et al., 2020). Nevertheless, the benefits of DI on reducing muskmelon cracking are less evaluated, and the cracking mechanisms of muskmelons associated to irrigation still remain mostly unclear. We hypothesized that DI would alleviate the cracking of muskmelons by acting on fruit growth, fruit cuticle strain, biomechanical properties and cell-wall metabolism. In this study, the objectives were to investigate the role of irrigation on fruit cracking based on cuticle development, biomechanics and cell-wall composition of pericarp in muskmelon. A better understanding of the fruit cracking mechanism will be helpful to making appropriate irrigation management practices.

2. Materials and methods

2.1. Experimental site

The experiment was conducted in a Venlo-type glass greenhouse of the Shiyanghe Experimental Station of China Agricultural University, located at Wuwei City, Gansu Province, Northwest China (37°52'N, 102°52'E, altitude 1581 m above sea level), from March to August in 2022. The environmental parameters (air temperature (Ta, °C), and relative humidity (RH, %) were monitored with the weather station (Hobo, Onset Computer Corp, USA) in the greenhouse. Ta, RH, and calculated vapor pressure deficit (VPD) during the whole growth period were shown in Fig. 1.

2.2. Experimental design

The cultivar “Tinglin” muskmelon (*Cucumis melo var. chinensis*), was used in the experiment. The fruit is elliptical with very thin and milky

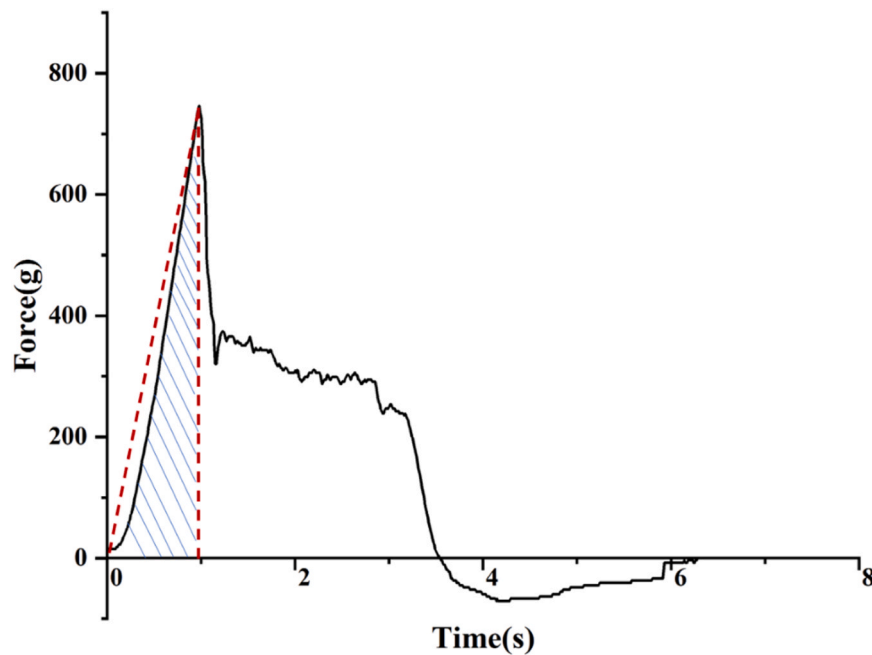


Fig. 2. The first peak of the curve represents the pericarp break force (g), ratio of the first peak and the running time represents the pericarp brittleness (g s^{-1}), the area between the curve of first peak and X-axis represents the pericarp toughness ($\text{g}\cdot\text{s}$).

green rind. The melon seeds were planted in plugs for germination on 19th March 2022, and transplanted at the four-leaf stage into matrix bags on 5th May 2022, which were filled with a mixed substrate containing coconut bran and coconut cake (1:1 v/v). One plant was potted per customized matrix bags and the main properties of the matrix bags were as follows: size, $23\text{ cm} \times 18\text{ cm} \times 12\text{ cm}$; weight, 1.07 kg; PH, 5.77; saturated volumetric moisture content, 0.78 gcm^{-3} .

Irrigation treatments began on 24th June, when the melons stepped into reproductive stage. The reproductive period of fruit growth is divided into two stages based on the fruit color change, including flowering and fruit development stage (Stage I, 0–18 days after full bloom (DAFB), the peel is green) and fruit maturation stage (Stage II, 19–28 DAFB, the peel changes from green to white). The daily amount of irrigation applied was calculated based on the actual daily evapotranspiration (ET), which was measured with a continuous weighing device (TCS-60, JingYanHengYe Technology Co., Ltd, Beijing). Three irrigation treatments were set as follow: the irrigation amount of T1 met the daily ET of the previous day, while mild and severe deficit irrigation treatments, referring as T2 and T3, respectively, received 75% and 50% of full irrigation amount of T1. The saturated paste conductivity (ECe) of groundwater used for irrigation was about 0.65 dS m^{-1} . The concentration of major ions such as K^+ , Na^+ , Mg^{2+} , Ca^{2+} , and Cl^- in groundwater were 9, 222, 61, 194, and 138 mg kg^{-1} , respectively (Jiang et al., 2012). Balanced water-soluble compound fertilizer (Nitrogen: Phosphorus: Potassium = 20: 20: 20) was applied every 2 or 3 days, with the same amount (average 0.15 g per plant each time) and timing of fertilizer application for all treatments. Melon plants were double-vine pruned to leave four fruits per plant. During the experimental period, except for irrigation, other management practices such as pollination, pruning branch stem, and pest control were the same for all treatments.

2.3. Parameters measurements

2.3.1. Rate of cracking

Four to five plants were selected with similar growth, no pests and diseases, and no picking during the experiment to determine the cracking rate. Fruit cracking rate was recorded by visually observing and counting the number of total and cracked fruits on the tagged branches

and converting the differential into a percentage: Cracking rate (%) = (Number of cracked fruit/Total number of fruit) \times 100%.

2.3.2. Plant water status

The fresh leaves were sampled to measure midday stem water potential (φ_{stem}) every 5–7 days using a pressure chamber (Model 1515D, PMS Instrument Company, USA). To allow equilibration with the stem, leaves were inserted in a black plastic bag covered by tin foil at least 60 min before the measurement (Rodriguez-Dominguez et al., 2022). φ_{stem} was measured between 12:30 p.m. and 13:30 p.m. In all cases, measurements were taken on four different individuals for each treatment.

2.3.3. Fruit growth

The muskmelon fruits were sampled every 5–7 days until harvest. Fresh weight (FW) was measured using an electronic balance (ME2002E, METTLER Toledo, Switzerland). The adjusted wrapping method was used to measure the surface area of the fruit (Villordon et al., 2020). Mass (surface area) increased rate was calculated by dividing the average value of mass (surface area) growth between adjacent samples by the interval days. Six fruits from three plants were sampled as replicates for each treatment.

2.3.4. Strain of the cuticle

The strain of the CM was determined based on the method reported by Knoche et al. (2004) and Lai et al. (2016). The evenly developed fruit without visual defects were selected and tagged. And point pattern composed of four marked points was placed at cheek region by toothpick between 5 DAFB and maturity. The initial distance between marked dots on the fruit surface in the transverse direction (perpendicular to the stem/stylar axis, x), and in longitudinal direction (parallel to the stem/stylar axis, y) were recorded by taking photos every 6 to 7 days, then quantified by image analysis (Image J, National Institutes of Health, USA). 6 to 7 days after printing the dots, fruit were transferred to the laboratory to quantify the final distance between each dot. Five fruits from three plants were sampled as replicates for each treatment.

Based on measurements taken using the dot patterns, uniaxial strain rates ($\varepsilon_t^x \text{ t}^{-1}$ and $\varepsilon_t^y \text{ t}^{-1}$ in $\text{mm mm}^{-1} \text{ day}^{-1}$ for horizontal and vertical

Table 1

Irrigation amount (I), evapotranspiration (ET) of single plant, midday stem water potential (ψ_{stem}) and fruits cracking rate in full irrigation (T1), mild deficit irrigation (T2), and severe deficit irrigation (T3).

Treatments	Stage I (0-18DAFB)		Stage II (19-28DAFB)		Total reproductive season		ψ_{stem} (Mpa)	Cracked fruit rate (%)
	I (L/plant)	ET (L/plant)	I (L/ plant)	ET (L/ plant)	I (L/plant)	ET (L/ plant)		
T1	19.58	18.43	8.68	8.63	28.26	27.06	-0.66 a	40.00 a
T2	14.98	16.21	6.2	5.7	21.17	21.91	-0.87 b	18.75 b
T3	9.32	13.15	4.38	4.33	13.69	17.48	-1.17 b	6.25 b

Note: The data of I and ET is calculated based on the weighing device data before and after irrigation. The value of ψ_{stem} is the average of twelve date from the whole reproductive growth stage. Different letters indicate significant difference among irrigation treatments at $P < 0.05$.

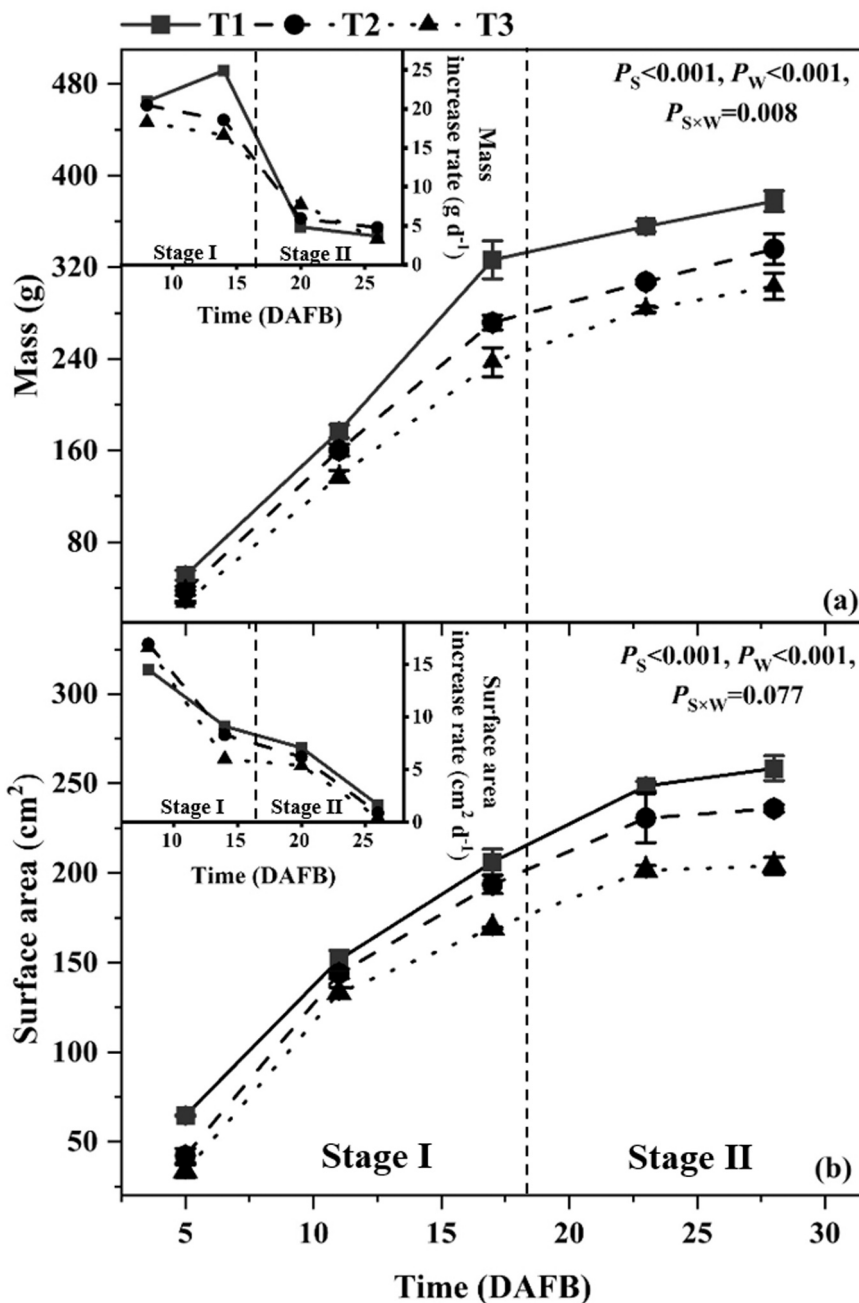


Fig. 3. Time course of change in fruit mass (n = 5) (a) and fruit surface area (n = 3) (b) between 5 and 28 days after full bloom (DAFB) under full irrigation (T1), mild deficit irrigation (T2), and severe deficit irrigation (T3). Inset: Rates of mass and surface area growth in the course of development. Values are means \pm SE. P values of two-way ANOVA for water (W) and stage (S) are shown in the table of each panel. The dotted line represents the boundary between the two stages.

direction, respectively) of the CM was calculated according to following equations.

$$\varepsilon_i^x t^{-1} = \frac{x - x_0}{x_0 * t} = \frac{\Delta x}{x_0 * t} \quad (1)$$

or

$$\varepsilon_i^y t^{-1} = \frac{y - y_0}{y_0 * t} = \frac{\Delta y}{y_0 * t} \quad (2)$$

In these equations, x and x_0 or y and y_0 represented the distance of dots at the time of application and sampling, respectively. t represented a given time interval for marking (6 or 7 days). The data for biaxial area strain (ε_i^{xy} in $\text{mm}^2 \text{mm}^{-2}$) was calculated from ε_i^x and ε_i^y using Eq. 3.

$$\varepsilon_i^{xy} = [(e_i^x + 1) * (e_i^y + 1)] - 1 = \frac{A - A_0}{A_0} = \frac{\Delta A}{A_0} \quad (3)$$

Dividing by t yielded the biaxial strains rates $\varepsilon_i^{xy} t^{-1}$.

2.3.5. Isolation of cuticular membranes and mass determination

The exocarp strips (5 mm × 10 mm) were sampled using a custom-made rectangular cutter. The CM was isolated enzymatically by incubating the exocarp strip in 50 mM citric acid-sodium citrate buffer solution (pH is 4.5) containing pectinase (0.2 g L⁻¹, Solarbio, Beijing, China), cellulase (0.6 g L⁻¹, Solarbio, Beijing, China), PC-300 liquid biological preservative (0.4 g L⁻¹, Solarbio, Beijing, China) to prevent microbial activity. Each time the enzyme solution was refreshed repeatedly until the CM complete separation from the tissue completely. The sample was washed thoroughly with deionized water. Whereafter, the CM was dried at 25 °C. The mass of the CM was determined by weighing a sample of CM ($n = 4$ or 5) with an analytical balance (ML104T/02, Mettler Toledo, Switzerland). CM mass per unit area was calculated by dividing mass of CM mass by the sampling area originally. As the exocarp of an intact muskmelon fruit was strained and sectioning fruit may release strain, only one strip was excised per fruit from the cheek region of muskmelon. CM mass of the whole fruit was calculated by multiplying average CM mass per unit area by average surface area each treatment. Six fruits from three plants were sampled as replicates for each treatment.

2.3.6. Biomechanical properties determination

The method was modified on the basis of biomechanical determination described by Li et al. (2018) and Zhang et al. (2023). Determination of mechanical properties of the muskmelon pericarp were achieved by the puncture test with texture analyzer (TMS Pro, FTC, The UK), which profiled a mechanical force displacement using a LA/P/2 cylindrical probe with a diameter of 2 mm. The parameters of the texture analyzer were adjusted to a test speed of 2.00 mm s⁻¹, posttest speed of 10.00 mm s⁻¹, test depth of 5.00 mm and auto force trigger of 5.00 g. Determination indices included the pericarp break force (g), pericarp brittleness (g s⁻¹) and pericarp toughness (g·s) (Fig. 2). Random points were selected on the fruit surface for testing. Three fruits from three plants were sampled as replicates for each treatment.

2.3.7. Determination of cell wall components

The protopectin and WSP content were determined with Multiskan Spectrum (Multiskan Go, ThermoFisher, U.S.A), using the protocols described by Wang et al. (2012). The content of cellulose and hemicellulose were determined with a fiber analyzer (Model ANKOM220, ANKOM Technology, U.S.A.) according to the method described by Naydenova and Vasileva (2015). Sampling occurred on the 11, 17, 23 and 28 DAFB after full bloom, respectively. Six fruits from three plants were sampled as replicates for each treatment.

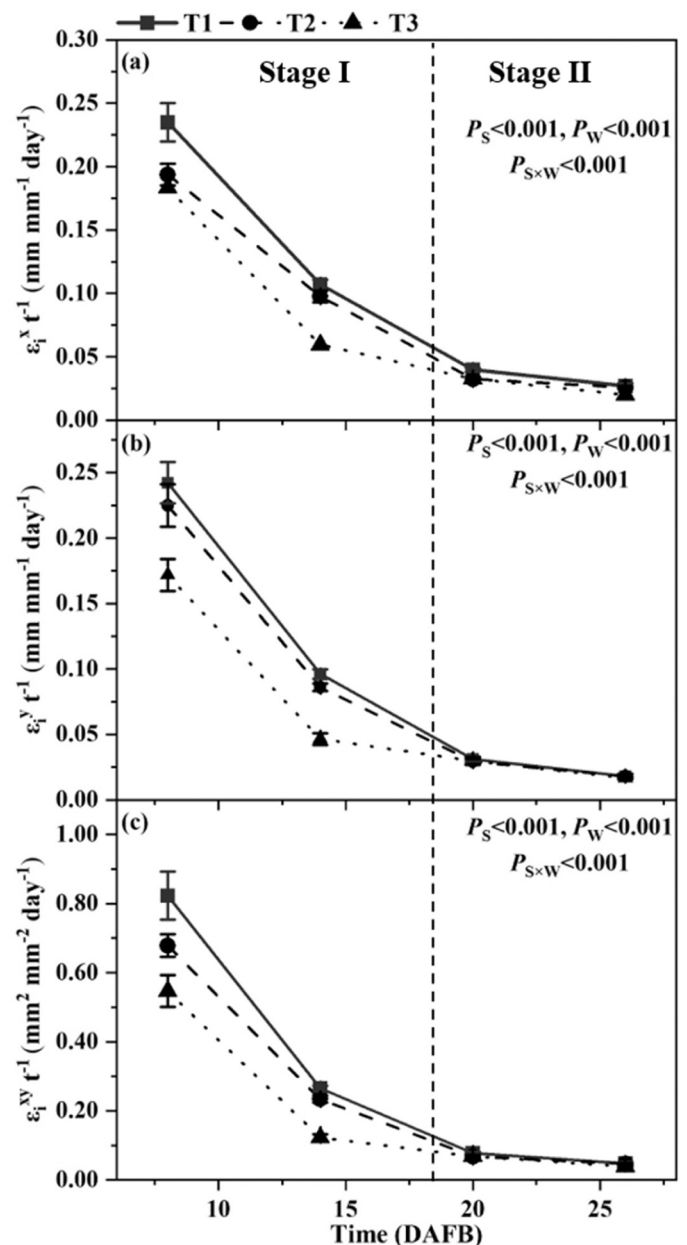


Fig. 4. Rates of total area strain ($\varepsilon_i^{xy} t^{-1}$) and of uniaxial strain in transverse (perpendicular to stem/stylar axis; $\varepsilon_i^x t^{-1}$) and longitudinal (parallel to stem/stylar axis; $\varepsilon_i^y t^{-1}$) direction of fruit surface between 5 and 28 days after full bloom (DAFB) under full irrigation (T1), mild deficit irrigation (T2), and severe deficit irrigation (T3). Values are means \pm SE ($n = 5$). P values of two-way ANOVA for water (W) and stage (S) are shown in the table of each panel. The dotted line represents the boundary between the two stages.

2.4. Statistical Analysis

The statistical software SPSS (Version 26.0; IBM Corp.) was used to analyze the variance of the test data. One-way ANOVA was performed to compare difference between treatments at each developmental stage. Two-way ANOVA was performed to test for the effects of water treatment, developmental stage, and their interaction.

A structural equation model (SEM) was conducted to quantify the causal pathways with the AMOS 21.0 (SPSS Inc., IBM Co., Armonk, NY, USA), in which melon growth (mass and surface area), cuticle, cell wall component (protopectin and hemicellulose), and biomechanical properties (pericarp break force, pericarp brittleness and pericarp toughness)

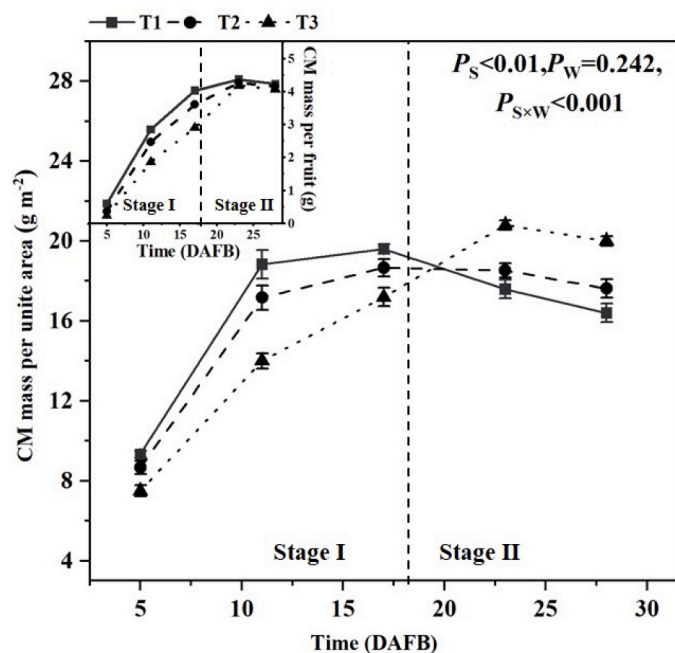


Fig. 5. Change in mass of cuticular membrane (CM) per unit area in the developing fruit between 5 and 28 days after full bloom (DAFB) under full irrigation (T1), mild deficit irrigation (T2), and severe deficit irrigation (T3). Inset: CM mass whole fruit in the course of development. Values are means \pm SE (n = 3). P values of two-way ANOVA for water (W) and stage (S) are shown in the table of each panel. The dotted line represents the boundary between the two stages.

were all involved. The one-way arrow associated with the coefficient represents the partial regression coefficient between two variables. The data were fitted to the models based on the maximum likelihood estimation. Model probability was assessed by χ^2 tests. In this regard, the final model was considered good fit with chi-square/degree values (CHI/DF) < 3, the applied comparative fit index (CFI) > 0.95, and the root mean square error of approximation (RMSEA) < 0.06 (Fan et al., 2016).

3. Results

3.1. Melon fruit cracking and growth were depressed by deficit irrigation

Table 1 showed the amount of evapotranspiration (ET) and irrigation water applied (I) at different growth stages for different treatments. ET was decreased by 19.03% and 35.40% under T2 and T3 compared to T1 for the whole growth stage, while φ_{stem} was reduced 31.81% and 77.27% in T2 and T3 respectively. The rate of fruit cracking was highest in T1 at 40%, but decreased by 53.13% and 84.38% in T2 and T3.

As shown in Fig. 3, fruit fresh mass and surface area increased during development. The growth trend was generally consistent among different treatments: there was a phase of rapid increase in mass and surface area at Stage I, followed by a plateau phase characterized by decreasing growth rates during mature period (Stage II). Generally, mass and surface area of muskmelon decreased with the irrigation amount. There was a significant stage \times water level interaction on mass ($P_{S \times W} = 0.008$, Fig. 3a), indicating that the sensitivity of fruit to water deficit was different for different stages. Compared with the T1, it was decreased by 26.52% and 45.91% under T2 and T3 in fruit mass at 5 DAFB, and the decreases in fruit surface area was 34.66% and 48.04%, respectively. By contrast, the fruit mass of T2 and T3 at 28 DAFB were lower by 11.06% and 19.67%, whilst the decreases in fruit surface area reached 8.69% and 21.06%, respectively. Meanwhile, the growth rate of fruit mass and surface area reached maximum at 5 to 17 DAFB and then declined until

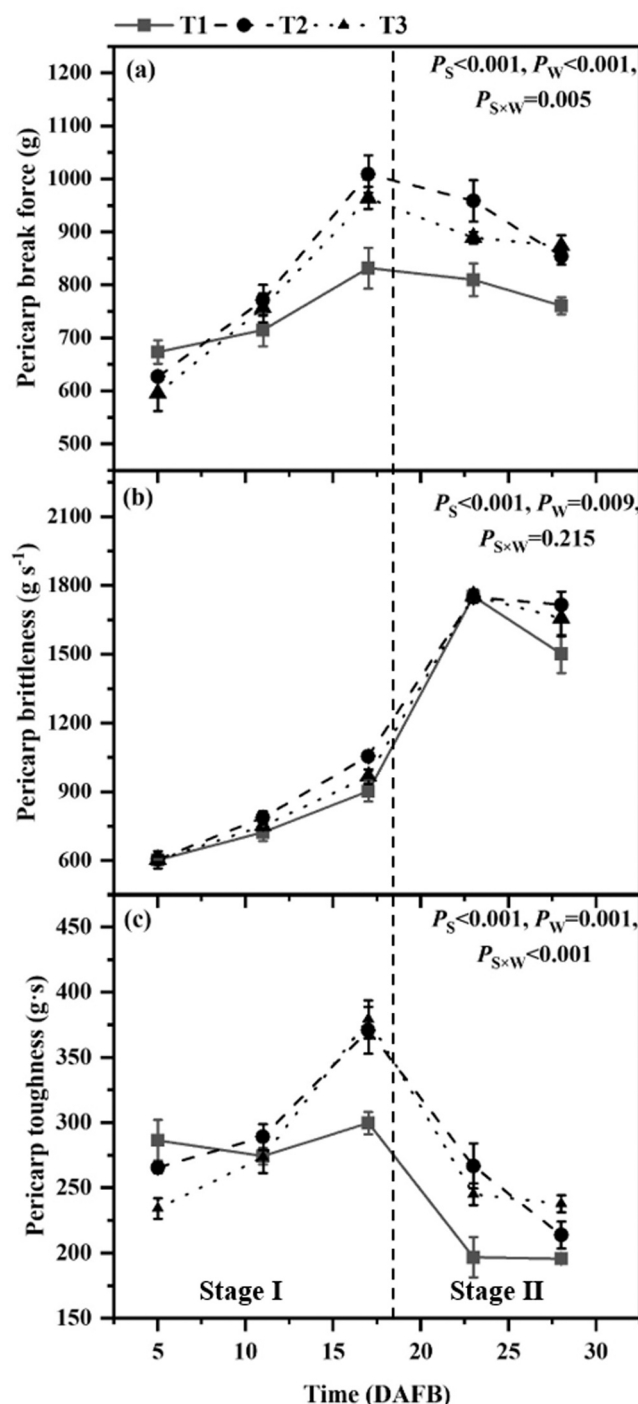


Fig. 6. The biomechanical performance of developing muskmelon fruit under full irrigation (T1), mild deficit irrigation (T2), and severe deficit irrigation (T3), including (a) pericarp break force, (b) pericarp brittleness and (c) pericarp toughness. Values are means \pm SE (n = 3). P values of two-way ANOVA for water (W) and stage (S) are shown in each panel. The dotted line represents the boundary between the two stages.

fruit mature.

3.2. Deficit irrigation induced slower strain rates during fruit development and higher CM mass per unit area at maturity

Significant interactions between stage and water supply were observed in both CM strain and mass ($P_{S \times W} < 0.001$, Figs. 4 and 5), indicating that the change of CM strain and mass under deficit irrigation

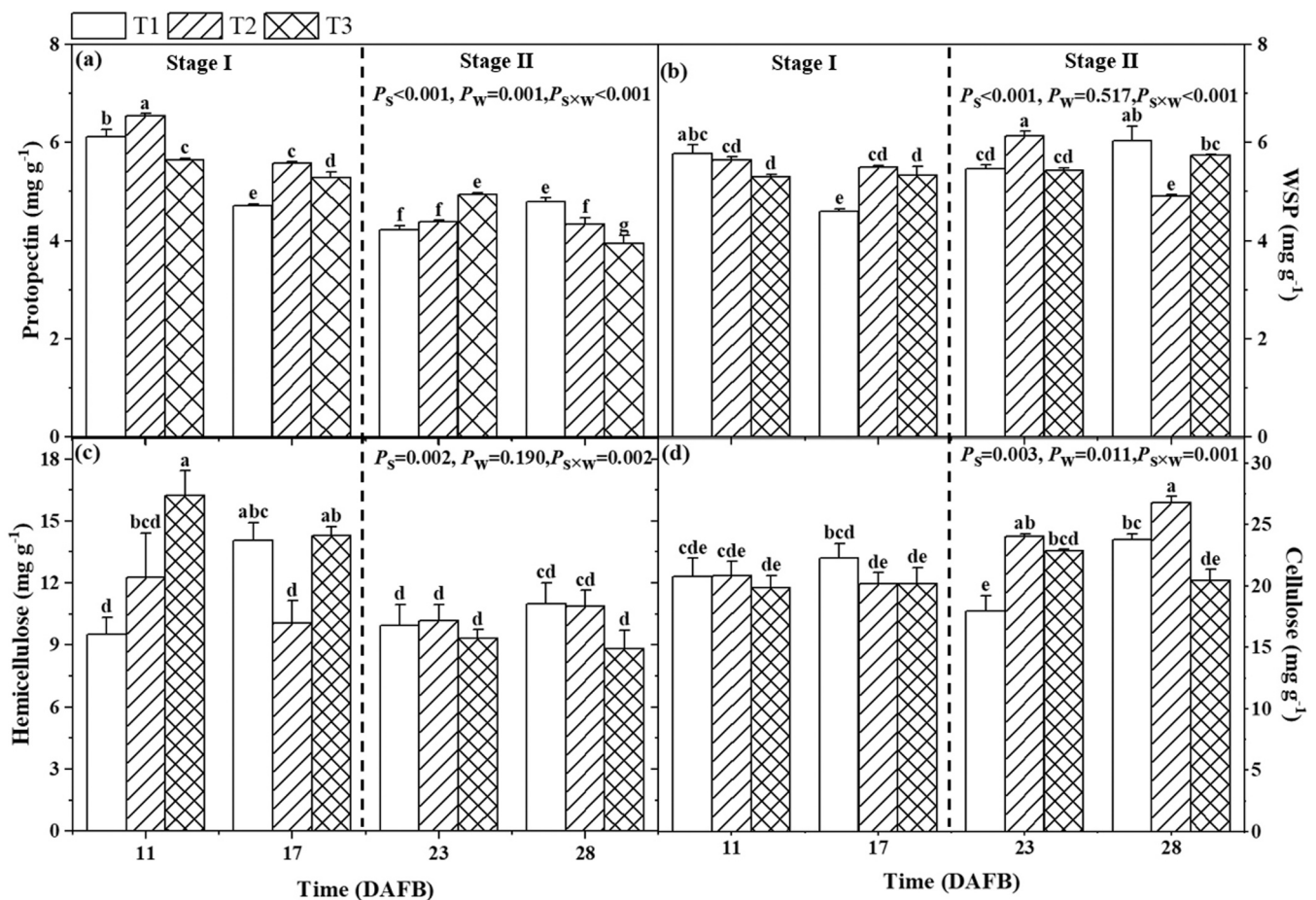


Fig. 7. The content of cell wall components of developing muskmelon fruit pericarp under full irrigation (T1), mild deficit irrigation (T2), and severe deficit irrigation (T3), including (a) protopectin, (b) water-soluble pectin (WSP), (c) cellulose, (d) hemicellulose. Values are means \pm SE ($n = 3$). P values of two-way ANOVA for water (W) and stage (S) are shown in each panel. Different letters indicate significant difference among irrigation treatments using Duncan's multiple range tests at $P = 0.05$ level.

were different during the development of muskmelon fruit. The rates of uniaxial strain ($\epsilon_x^x t^{-1}$ and $\epsilon_y^y t^{-1}$) and biaxial area strain ($\epsilon^{xy} t^{-1}$) of the fruit surface had same tendency with the highest strain rate at the initial stage and decreasing to nil towards the maturity. Compare with T1, $\epsilon_x^x t^{-1}$, $\epsilon_y^y t^{-1}$ and $\epsilon^{xy} t^{-1}$ from 11 to 17 DAFB decreased by 44.30%, 51.65%, and 53.61% under T3 respectively, while the reduction was reduced to 26.02%, 6.68% and 19.18% in the final days, respectively.

The CM mass of the whole fruit increased up to 23 DAFB with the highest deposition rates during early development stage. Fig. 5 showed that the mass of CM per unit area of muskmelon fruit increased at Stage I for all the treatments, but decreased in T1 and T2 from 18DAFB. At Stage I, the CM mass per unit area was significantly higher for T1 than other treatments. However, the content of CM mass per unit area in T1 decreased quickly when fruit stepped into the maturity. In contrast to T1, more CM was synthesized under deficit water conditions during mature period.

3.3. Deficit irrigation caused the better pericarp cracking force, pericarp brittleness and pericarp toughness

The changes of the pericarp break force were similar for all treatments throughout the development process. The pericarp break force increased with fruit development at Stage I, and then decreased at Stage II (Fig. 6a). The pericarp brittleness gradually increased at Stage I, then dramatically increased after entering Stage II followed by a downward trend near harvest (Fig. 6b). The pericarp toughness first increased to the maximum before entering Stage II and then decreased (Fig. 6c).

There was a significant difference between the three irrigation treatments on the pericarp break force, pericarp brittleness and pericarp toughness. In addition, significant interactions between stage and water level were observed in the pericarp break force ($P_{s \times w} = 0.005$, Fig. 6a) and pericarp toughness ($P_{s \times w} < 0.001$, Fig. 6c). T1 had the maximum fruit breaking force and pericarp toughness at 5 DAFB. However, deficit irrigation had marked positive effects on pericarp cracking force, pericarp brittleness and pericarp toughness during fruit growth and maturation.

3.4. Mild deficit irrigation had significantly higher cellulose content and lower WSP content at fruit maturation stage

There were significant changes in the cell wall fractions of the pericarp of developing fruits (Fig. 7). Compared to Stage I, the content of protopectin and hemicelluloses at Stage II decreased. However, the water-soluble pectin (WSP) content and cellulose of pericarp showed a reverse trend. Multiple comparisons indicated that there was significant interaction between irrigation level and development stage in protopectin ($P_{s \times w} < 0.001$, Fig. 7a), WSP ($P_{s \times w} < 0.001$, Fig. 7b), hemicelluloses ($P_{s \times w} = 0.002$, Fig. 7c), and cellulose ($P_{s \times w} = 0.001$, Fig. 7d). In general, T2 had the highest protopectin content, while the highest content of hemicellulose obtained by T3 at Stage I. By comparison, there was significantly higher cellulose content and lower WSP content in T2 compared with full irrigation in the last stage. However, T3 had the lowest content in protopectin, and cellulose at 28 DAFB. There was no significant difference in hemicellulose content among the

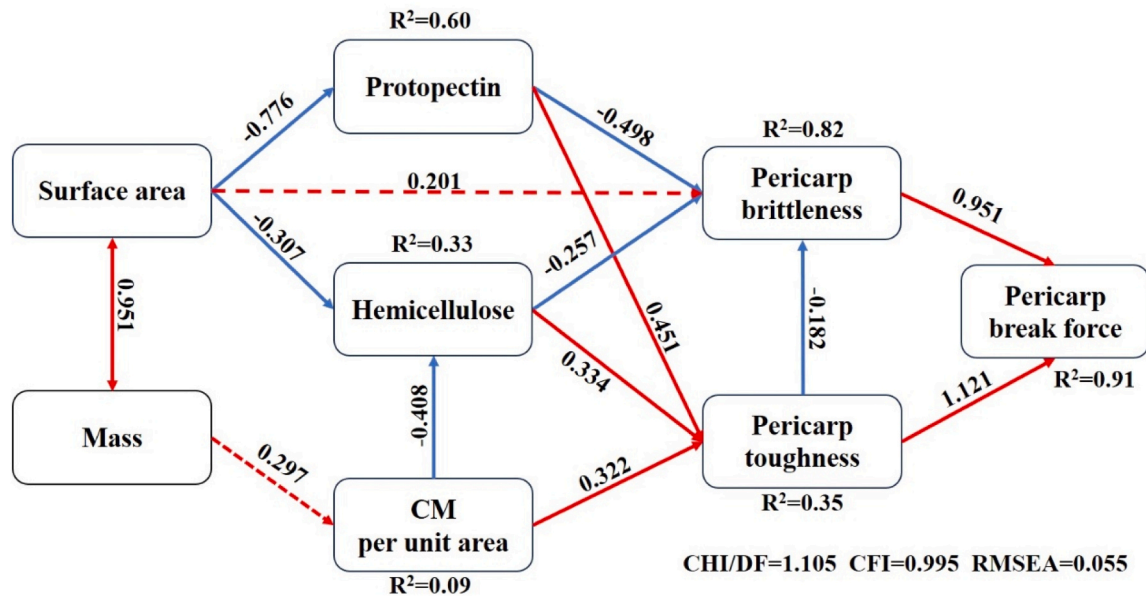


Fig. 8. Structural equation model (SEM) on fruit mass, surface area, CM per unit area, protopectin, hemicellulose, pericarp break force, pericarp brittleness and pericarp toughness. Arrows indicate the proposed links between variables. The red and blue arrows indicate negative and positive correlations, respectively, whereas solid lines and dashed lines indicate significant paths ($p < 0.05$) and non-significant paths, respectively. Standardized path coefficients are shown on the arrows. The R^2 values indicate the percentage of variance explained by the relationships with other variables. Goodness-of-fit statistics are shown underneath the modeling frames.

treatments at Stage II.

3.5. Fruit growth affected biomechanical properties through the cuticle and cell wall components

Structural equation model (SEM) results manifested the speculative causal relationships among fruit development, cuticle, cell wall components and biomechanical properties of melon (Fig. 8). There was a significant positive correlation between surface area and mass ($\lambda = 0.951$, $P < 0.001$). Surface area was negatively correlated with protopectin ($\lambda = -0.776$, $P < 0.001$) and hemicellulose ($\lambda = -0.307$, $P = 0.032$), but the indirect effect of surface area on pericarp brittleness was not significant ($\lambda = 0.201$, $P = 0.109$). The direct impact of fruit mass on CM per unit area was not significant ($\lambda = 0.297$, $P = 0.066$). Protopectin and hemicellulose were significantly negatively correlated with pericarp brittleness ($\lambda = -0.498$, $P < 0.001$; $\lambda = -0.257$, $P = 0.001$), but highly positively correlated with pericarp toughness ($\lambda = 0.451$, $P = 0.002$; $\lambda = 0.334$, $P = 0.036$). CM per unit area had a significant positive effect on pericarp toughness ($\lambda = 0.322$, $P = 0.043$). Pericarp toughness showed a significant negative effect on pericarp brittleness ($\lambda = -0.182$, $P = 0.037$). Pericarp break force was significantly influenced by the direct positive effect of pericarp brittleness ($\lambda = 0.951$, $P < 0.001$) and pericarp toughness ($\lambda = 1.121$, $P < 0.001$).

4. Discussion

We investigated the relationship between irrigation and melon cracking by analyzing the impact of irrigation on the fruit growth, cuticle, biomechanics and cell wall components during the muskmelon development. Overall, mild deficit irrigation was a reasonable practical strategy that could greatly alleviate fruit cracking by slightly reducing fruit growth, decreasing cuticle strain, and improving the biomechanical properties of pericarp by regulating cell wall metabolism (Fig. 8, Fig. 9). Our research provided a new insight for irrigation management to reduce fruit cracking.

4.1. Deficit irrigation decreased fruit cracking by regulating fruit growth

Cultural management practices such as tree spacing, pruning, fruit thinning and irrigation, are crucial factors influencing the occurrence and intensity of cracking (Gilbert et al., 2007). Among these, irrigation is the most intensively practiced operation throughout the growing season, and plays an irreplaceable role in fruit cracking. In the present study, low irrigation reduced stem water potential at midday (Table 1), a reliable indicator of plant water status (Boini et al., 2019), which represents a limitation of water transport from the plant to the fruit (Measham et al., 2010; Li et al., 2021b). The decrease of fruit water accumulation would help to decrease the internal pressure of fruit, which is considered as being the cause of the decrease in susceptibility to cracking and skin failure (Considine and Kriedemann, 1972).

Fruit cracking and splitting have been partly attributed to the unreasonable irrigation management (Kong et al., 2013). In this study, we found that although deficit irrigation (T2) decreased fruit mass by about 11.06%, a more pronounced decrease in fruit cracking was achieved (by about 53.13%), thus avoiding a dramatic economic loss (Table 1), which were consistent with previous studies on tomatoes (Peet and Willits, 1995), nectarine (Gilbert et al., 2007), and figs (Kong et al., 2013). Both mass and surface area of muskmelon growth followed sigmoid patterns with time (Fig. 3). Notably, there was slow change in mass while surface area increased rapidly in the prophase of Stage II (Fig. 3), which meant dramatic strain imposed on the pericarp, causing greater risk of skin failure (Ginzberg and Stern, 2019). In addition, fruit cracking susceptibility could be related to a higher growth rate (Domínguez et al., 2012). In this study, the highest area expansion rate and the maximum mass increase rate were observed under higher water supply (Fig. 3). Deficit irrigation resulted in a significant decrease in the fruit growth and tissue expansion (Fig. 3), which further supported that DI influenced fruit growth by decreasing its rate, thus playing a positive role in alleviating cracking.

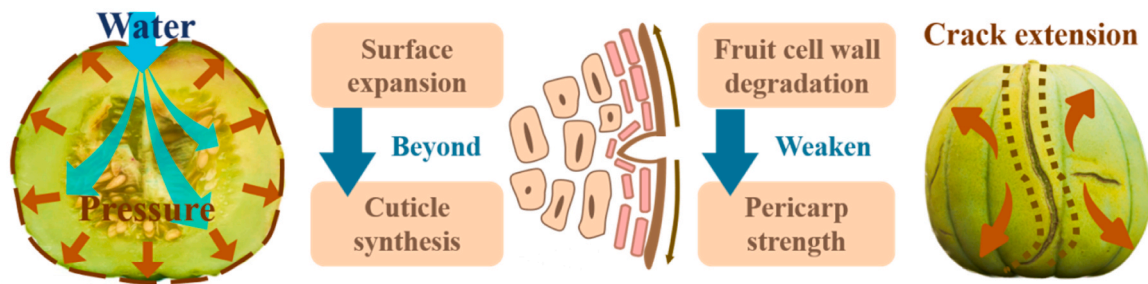


Fig. 9. During growth and development of muskmelon, the increase of surface area in the absence of cuticle deposition and changes of biomechanical properties of pericarp due to that cell wall degradation may cause cuticle tension and microcracks formation. Microcracks extend and eventually develop into macroscopic cracks.

4.2. The development pattern of the CM affects fruit cracking

Although the strain rate decreased as the muskmelon developed, the cuticle was constantly stretched. The decrease of CM mass per unit area and constant CM mass on a whole fruit of muskmelon occurred at Stage II (Fig. 5), which would be expected based on its fruit surface expansion after cessation of CM deposition. This indicated that the CM was subject to great plastic and elastic strain. It is noteworthy that elastic behavior would result in an increased risk of CM fracture (Knoche et al., 2004). Differences in the ratio of CM deposition and fruit surface expansion during growth result in the development of stresses to a continuously thinning CM, leading to the formation of microcracks (Peschel et al., 2007). The cracks on the CM of the pericarp reduce the protective barrier function of the CM and further lead to fruit cracking. It was reported that irrigation levels could affect fruit CM thickness (Pérez-Pastor et al., 2007), and a thicker CM may have been caused by deficit irrigation on fruit (Blanco et al., 2019). Cuticular biosynthesis is an adaptive mechanism to resist drought (Tafolla-Arellano et al., 2018). In this study, we found that high irrigation amount led to thinner CM (Fig. 4, Fig. 5), which may be due to lower CM synthesis and faster fruit growth rate at maturity (Tafolla-Arellano et al., 2018; Li et al., 2020). Excess water within fruit could promote the occurrence of cuticular cracks, and then macroscopic cracks by acting on CM strain, as it has been described by Gilbert et al. (2007).

In the case of muskmelon, fruit cracking occurs at the late stage of ripening when the synthesis of CM almost terminated. There may be a relationship between the synthesis of CM and the crack susceptibility stage at which fruits are more prone to cracking (Domínguez et al., 2011). CM are substantially accumulated at maturity in tomato (Bargel and Neinhuis, 2005), apple (Lai et al., 2016) and Jujube (Li et al., 2018), whereas crack initiation can occur throughout the entire period of fruit development and ripening. By contrast, it has been reported that cherry tomato (Domínguez et al., 2008) and sweet cherry fruit (Knoche et al., 2004) accumulate CM at the early stage of fruit development, and cracking problem only occur during the ripening process (Domínguez et al., 2011), which is similar to the pattern of muskmelon in this study. However, it is necessary to further explore the intrinsic mechanism of the differences in the formation of CM between different fruits at the molecular level.

4.3. Mild deficit irrigation affects fruit cracking by modifying biomechanical properties and cell wall metabolism of pericarp

The mechanical performance of the fruit skin is considerably prominent for the integrity of the whole fruit, playing a significant role in fruit appearance and storage (Bargel and Neinhuis, 2005). In particular, the pericarp break force reflects the peel strength, and the toughness indicates the energy required to break the peel of intact fruit (Sirisomboon et al., 2012), both of which are considered to be related to fruit cracking (Li et al., 2018). In this study, both of the pericarp break force and pericarp toughness of muskmelon decreased at Stage II (Fig. 6), indicating that fruit was more prone to cracking during fruit maturation. The

same properties were also found in pears (Sirisomboon et al., 2000) and tomato (Sirisomboon et al., 2012). It has been reported that the change in mechanical properties may be related to the loose cuticle and waxy layer falling off on the surface of the pericarp after entering the mature stage, increased risk of cracking (Li et al., 2018). In this study, we found that the CM mass per unit area, the pericarp break force and pericarp toughness all showed a decrease tendency after entering the mature stage (Fig. 5, Fig. 6). Studies have shown that excessive irrigation stimulated cell expansion, leading to an increase in cell volume and a deterioration in pericarp biomechanical properties, and eventually pericarp cracking (Brüeggewirth and Knoche, 2017; Li et al., 2023). Our study showed that the lower pericarp break force, pericarp brittleness, and pericarp toughness under high irrigation (Fig. 6), which was consistent with the results that high irrigation amount had negative effects on peel strength and skin break force (Peet, 1992; Fernandes et al., 2015).

Cell wall also plays a vital role in the mechanical properties of pericarp, thus in fruit cracking (Jiang et al., 2019; Forlani et al., 2019). Cell wall not only supports the cells, but is also responsible for cell adhesion. The degradation of cell wall substances during fruit development is a characteristic of the fruit-ripening process (Yakushiji et al., 2001), which render the fruit less rigid and structurally weaker. The change in cell wall components during maturation is associated with cell-wall-related degrading enzyme activities and cell wall gene expression levels enhancement (Posé et al., 2019). It has been reported that cell wall disintegration degree and cracking susceptibility both increase during the fruit development (Farquhar and Zhao, 2006). Furthermore, the cell wall mechanical structure of cracked fruits is weaker with stronger cell-wall-metabolism (Jiang et al., 2022). The cellulose fraction contributes to the rigidity of structure, and cell wall plasticity and viscoelasticity rely on the pectin and hemicellulose (Schumann et al., 2020). In this study, the content of protopectin and hemicellulose of muskmelon decreased, while the WSP content increased with fruit growth (Fig. 7), which may be a good explanation for the change of mechanical properties of muskmelons (Fig. 8). Irrigation has been shown to modify the mechanical properties of fruits by cell wall composition and wall-modifying enzyme activities, thus changing the biomechanical properties of fruit textural (Diarte et al., 2022). It has been reported that the cellulose content of fruits decreases with increasing irrigation (Chen et al., 2022), and water deficit could help to maintain the pectin levels (Fernandes et al., 2015). However, severe deficit irrigation results in weakened anabolism and enhanced catabolism in plants, which may be a reason for rapid cell wall decomposition (Cossani and Reynolds, 2012). In agreement with those previous experimental results, our study indicates that better biomechanical performance under mild deficit irrigation treatments might relate to the slower cell wall degradation (Fig. 7).

5. Conclusions

The inflow of water into fruits results in heightened internal pressure, causing pericarp stress. Meanwhile, during muskmelon fruit

growth and ripening, the change of morphology, the mechanical properties, and cell wall metabolism of fruit weakens the cracking resistant of fruit peel, ultimately leading to the generation and extension of cracks. Severe fruit cracking occurred under full irrigation conditions, which produced higher fruit growth rate, worse biomechanical properties and unfavorable cell wall structure. Mild deficit irrigation could decrease the incidence of fruit cracking in muskmelon while also reducing water use, which could be related with the decreased strain of cuticle and the increased pericarp break force and toughness induced by the cell wall metabolism. Whilst the lowest fruit cracking rate was attained under severe water deficit, it also resulted in the smallest fruit mass and surface area, as well as rapid decomposition of cell walls, which impeded fruit growth and quality. Hence, mild water deficit emerges as an efficient approach to alleviate fruit cracking. From the perspective of integrated horticultural production, further work is needed to consider the economic benefit and fruit quality based on comprehensive impact of irrigation on fruit cracking.

CRedit authorship contribution statement

Xue Qimin: Writing – original draft, Investigation, Conceptualization. **Li Hao:** Writing – review & editing, Validation. **Chen Jinliang:** Writing – review & editing, Validation. **Du Taisheng:** Writing – review & editing, Validation, Supervision, Funding acquisition.

Declaration of Competing Interest

The authors declare that they have no known competing financial interests or personal relationships that could have appeared to influence the work reported in this paper.

Data availability

Data will be made available on request.

Acknowledgements

We appreciate the valuable comments by Dr. Chuanbin Liang on diagrams of this manuscript. This work was supported by research grants from the National Natural Science Foundation of China (52239002) and the National Key Research and Development Program of China (2022YFD1900500).

References

- Bargel, H., Neinhuis, C., 2005. Tomato (*Lycopersicon esculentum* mill.) Fruit growth and ripening as related to the biomechanical properties of fruit skin and isolated cuticle. *J. Exp. Bot.* 56, 1049–1060 <https://doi.org/10.1093/jxb/eri098>.
- Blanco, V., Torres-Sánchez, R., Blaya-Ros, P.J., Pérez-Pastor, A., Domingo, R., 2019. Vegetative and reproductive response of 'prime giant' sweet cherry trees to regulated deficit irrigation. *Sci. Hortic.* 249, 478–489. <https://doi.org/10.1016/j.scienta.2019.02.016>.
- Boini, A., Manfrini, L., Bortolotti, G., Corelli-Grappadelli, L., Morandi, B., 2019. Monitoring fruit daily growth indicates the onset of mild drought stress in apple. *Sci. Hortic.* 256, 108520 <https://doi.org/10.1016/j.scienta.2019.05.047>.
- Brown, K., Considine, J., 1982. Physical aspects of fruit growth. Stress distribution around lenticels. *Plant Physiol.* 69, 585–590 <https://doi.org/10.1104/pp.69.3.585>.
- Brüeggewirth, M., Knoche, M., 2017. Cell wall swelling, fracture mode, and the mechanical properties of cherry fruit skins are closely related. *Planta* 245, 765–777 <https://doi.org/10.1007/s00425-016-2639-7>.
- Chang, B., Zhang, Y., Keller, M., 2019. Softening at the onset of grape ripening alters fruit rheological properties and decreases splitting resistance. *Planta* 250, 1293–1305 <https://doi.org/10.1007/s00425-019-03226-y>.
- Chen, F., Cui, N., Jiang, S., Li, H., Wang, Y., Gong, D., Hu, X., Zhao, L., Liu, C., Qiu, R., 2022. Effects of water deficit at different growth stages under drip irrigation on fruit quality of citrus in the humid areas of south China. *Agric. Water Manag.* 262, 107407 <https://doi.org/10.1016/j.agwat.2021.107407>.
- Considine, J.A., Kriedemann, P.E., 1972. Fruit splitting in grapes. Determination of the critical turgor pressure. *Aust. J. Agric. Res.* 23, 17–23 <https://doi.org/10.1071/AR9720017>.
- Cossani, C.M., Reynolds, M.P., 2012. Physiological traits for improving heat tolerance in wheat. *Plant Physiol.* 160, 1710–1718 <https://doi.org/10.1104/pp.112.207753>.
- Cybulska, J., Zdunek, A., Konstankiewicz, K., 2011. Calcium effect on mechanical properties of model cell walls and apple tissue. *J. Food Eng.* 102, 217–223. <https://doi.org/10.1016/j.jfoodeng.2010.08.019>.
- Deng, J., Shi, Z., Li, X., Liu, H., 2013. Effects of cold storage and 1-methylcyclopropene treatments on ripening and cell wall degrading in rabbiteye blueberry (*Vaccinium ashei*) fruit. *Food Sci. Technol. Int* 20, 287–298 <https://doi.org/10.1177/1082013213483611>.
- Diarte, C., Iglesias, A., Graell, J., Lara, I., 2022. Firmness and cell wall changes during maturation of 'arbequina' olive fruit: the impact of irrigation. *Horticulturae* 8, 872. <https://doi.org/10.3390/horticulturae8100872>.
- Domínguez, E., Lopez-Casado, G., Cuartero, J., Heredia, A., 2008. Development of fruit cuticle in cherry tomato (*Solanum lycopersicum*). *Funct. Plant Biol.* 35, 403–411 <https://doi.org/10.1071/FP08018>.
- Domínguez, E., Cuartero, J., Heredia, A., 2011. An overview on plant cuticle biomechanics. *Plant Sci.* 181, 77–84. <https://doi.org/10.1016/j.plantsci.2011.04.016>.
- Domínguez, E., Fernández, M.D., Hernández, J.C.L., Parra, J.P., España, L., Heredia, A., Cuartero, J., 2012. Tomato fruit continues growing while ripening, affecting cuticle properties and cracking. *Physiol. Plant.* 146, 473–486. <https://doi.org/10.1111/j.1399-3054.2012.01647.x>.
- Du, T.S., Kang, S.Z., Zhang, J.H., Davies, W.J., 2015. Deficit irrigation and sustainable water-resource strategies in agriculture for china's food security. *J. Exp. Bot.* 66, 2253–2269 <https://doi.org/10.1093/jxb/erv034>.
- Fan, Y., Chen, J., Shirkey, G., John, R., Wu, S.R., Park, H., Shao, C., 2016. Applications of structural equation modeling (SEM) in ecological studies: an updated review. *Ecol. Process* 5, 19 <https://doi.org/10.1186/s13717-016-0063-3>.
- Farquhar, T., Zhao, Y., 2006. Fracture mechanics and its relevance to botanical structures. *Am. J. Bot.* 93, 1449–1454 <https://doi.org/10.3732/ajb.93.10.1449>.
- Fernandes, J.C., Cobb, F., Tracana, S., Costa, G.J., Valente, L., Goulao, L.F., Amâncio, S., 2015. Relating water deficiency to berry texture, skin cell wall composition, and expression of remodeling genes in two *Vitis vinifera* L. Var. *J. Agric. Food Chem.* 63, 3951–3961 <https://doi.org/10.1021/jf505169z>.
- Forlani, S., Masiero, S., Mizzotti, C., 2019. Fruit ripening: the role of hormones, cell wall modifications, and their relationship with pathogens. *J. Exp. Bot.* 70, 2993–3006 <https://doi.org/10.1093/jxb/erz112>.
- Gilbert, C., Chadoeuf, J., Vercambre, G., Genard, M., Lescouret, F., 2007. Cuticular cracking on nectarine fruit surface: spatial distribution and development in relation to irrigation and thinning. *J. Am. Soc. Hortic. Sci.* 132, 583–591 <https://doi.org/10.21273/JASHS.132.5.583>.
- Ginzberg, I., Stern, R.A., 2019. Control of fruit cracking by shaping skin traits – apple as a model. *Crit. Rev. Plant Sci.* 38, 401–410. <https://doi.org/10.1080/07352689.2019.1698129>.
- Grimm, E., Hahn, J., Pflugfelder, D., Schmidt, M.J., van Dusschoten, D., Knoche, M., 2019. Localized bursting of mesocarp cells triggers catastrophic fruit cracking. *Hortic. Res.* 6, 79 <https://doi.org/10.1038/s41438-019-0161-3>.
- Hou, X., Zhang, W., Du, T., Kang, S., Davies, W.J., 2020. Responses of water accumulation and solute metabolism in tomato fruit to water scarcity and implications for main fruit quality variables. *J. Exp. Bot.* 71, 1249–1264 <https://doi.org/10.1093/jxb/erz526>.
- Jiang, F., Lopez, A., Jeon, S., de Freitas, S.T., Yu, Q., Wu, Z., Labavitch, J.M., Tian, S., Powell, A.L.T., Mitcham, E., 2019. Disassembly of the fruit cell wall by the ripening-associated polygalacturonase and expansin influences tomato cracking. *Hortic. Res.* 6, 17 <https://doi.org/10.1038/s41438-018-0105-3>.
- Jiang, J., Huo, Z., Feng, S., Zhang, C., 2012. Effect of irrigation amount and water salinity on water consumption and water productivity of spring wheat in northwest China. *Field Crops Res.* 137, 78–88. <https://doi.org/10.1016/j.fcr.2012.08.019>.
- Jiang, Y., Yin, H., Wang, D., Zhong, Y., Deng, Y., 2022. Exploring the mechanism of akebia trifoliata fruit cracking based on cell-wall metabolism. *Food Res. Int.* 157, 111219 <https://doi.org/10.1016/j.foodres.2022.111219>.
- Khanal, B.P., Grimm, E., Knoche, M., 2011. Fruit growth, cuticle deposition, water uptake, and fruit cracking in jostaberry, gooseberry, and black currant. *Sci. Hortic.* 128, 289–296. <https://doi.org/10.1016/j.scienta.2011.02.002>.
- Knoche, M., Beyer, M., Peschel, S., Oparlak, B., Bukovac, M.J., 2004. Changes in strain and deposition of cuticle in developing sweet cherry fruit. *Physiol. Plant.* 120, 667–677 <https://doi.org/10.1111/j.0031-9317.2004.02855.x>.
- Kong, M., Lampinen, B., Shackel, K., Crisosto, C.H., 2013. Fruit skin side cracking and ostiole-end splitting shorten postharvest life in fresh figs (*Ficus carica* L.). But are reduced by deficit irrigation. *Postharvest Biol. Technol.* 85, 154–161. <https://doi.org/10.1016/j.postharvbio.2013.06.004>.
- Lai, X., Khanal, B.P., Knoche, M., 2016. Mismatch between cuticle deposition and area expansion in fruit skins allows potentially catastrophic buildup of elastic strain. *Planta* 244, 1145–1156 <https://doi.org/10.1007/s00425-016-2572-9>.
- Li, D., Li, Z., Tchuente-Magaia, F., 2021a. An extended finite element model for fracture mechanical response of tomato fruit. *Postharvest Biol. Technol.* 174, 111468 <https://doi.org/10.1016/j.postharvbio.2021.111468>.
- Li, D., Liu, Y., Fadji, T., Li, Z., Okasha, M., 2023. Analysis of the correlation between mesocarp biomechanics and its cell turgor pressure: a combined fem-dem investigation for irrigation-caused tomato cracking. *J. Texture Stud.* 54, 206–221. <https://doi.org/10.1111/jtxs.12720>.
- Li, H., Zhang, X., Hou, X., Du, T., 2021b. Developmental and water deficit-induced changes in hydraulic properties and xylem anatomy of tomato fruit and pedicels. *J. Exp. Bot.* 72, 2741–2756 <https://doi.org/10.1093/jxb/erab001>.
- Li, N., Song, Y., Li, J., Chen, Y., Xue, X., Li, L., 2018. Development of the cuticular membrane and biomechanical properties in hupingzao (*Ziziphus jujuba* mill. 'hupingzao'). *Sci. Hortic.* 229, 25–32. <https://doi.org/10.1016/j.scienta.2017.09.019>.

- Li, N., Fu, L., Song, Y., Li, J., Xue, X., Li, S., Li, L., 2020. Wax composition and concentration in jujube (*Ziziphus jujuba mill.*) Cultivars with differential resistance to fruit cracking. *J. Plant Physiol.* 255, 153294 <https://doi.org/10.1016/j.jplph.2020.153294>.
- Liao, N., Hu, Z., Li, Y., Hao, J., Chen, S., Xue, Q., Ma, Y., Zhang, K., Mahmoud, A., Ali, A., Malangisha, G.K., Lyu, X., Yang, J., Zhang, M., 2020. Ethylene-responsive factor 4 is associated with the desirable rind hardness trait conferring cracking resistance in fresh fruits of watermelon. *Plant Biotechnol. J.* 18, 1066–1077. <https://doi.org/10.1111/pbi.13276>.
- Lichter, A., Dvir, O., Fallik, E., Cohen, S., Golan, R., Shemer, Z., Sagi, M., 2002. Cracking of cherry tomatoes in solution. *Postharvest Biol. Technol.* 26, 305–312. [https://doi.org/10.1016/S0925-5214\(02\)00061-3](https://doi.org/10.1016/S0925-5214(02)00061-3).
- Lopez-Zaplana, A., Bárzana, G., Agudelo, A., Carvajal, M., 2020. Foliar mineral treatments for the reduction of melon (*Cucumis melo L.*) Fruit cracking. *Agronomy* 10, 1815. <https://doi.org/10.3390/agronomy10111815>.
- Lopez-Zaplana, A., Bárzana, G., Ding, L., Chaumont, F., Carvajal, M., 2022. Aquaporins involvement in the regulation of melon (*Cucumis melo L.*) Fruit cracking under different nutrient (ca, b and zn) treatments. *Environ. Exp. Bot.* 201, 104981 <https://doi.org/10.1016/j.envexpbot.2022.104981>.
- Measham, P.F., Gracie, A.J., Wilson, S.J., Bound, S.A., 2010. Vascular flow of water induces side cracking in sweet cherry (*Prunus avium L.*). *Adv. Hortic. Sci.* 24, 243–248 (<https://go.exlibris.link/CLKMCDnM>).
- Naydenova, Y., Vasileva, V., 2015. Forage quality analysis of perennial legumes-subterranean clover mixtures. *Sci. Int.* 3, 113–120 <https://10.17311/sciintl.2015.113.120>.
- Opara, L.U., Hodson, A.J., Studman, C.J., 2000. Stem-end splitting and internal ring-cracking of 'gala' apples as influenced by orchard management practices. *J. Hortic. Sci. Biotechnol.* 75, 465–469 <https://10.1080/14620316.2000.11511270>.
- Peet, M.M., 1992. Fruit cracking in tomato. *HortTech* 2, 216–223 <https://10.21273/HORTTECH.2.2.216>.
- Peet, M.M., Willits, D.H., 1995. The role of excess water in tomato fruit cracking. *HortSci*, 30, 65–68 <https://10.21273/HORTSCI.30.1.65>.
- Pérez-Pastor, A., Ruiz-Sánchez, M.C., Martínez, J.A., Nortes, P.A., Artés, F., Domingo, R., 2007. Effect of deficit irrigation on apricot fruit quality at harvest and during storage. *J. Sci. Food Agric.* 87, 2409–2415. <https://doi.org/10.1002/jsfa.2905>.
- Peschel, S., Franke, R., Schreiber, L., Knoche, M., 2007. Composition of the cuticle of developing sweet cherry fruit. *Phytochemistry* 68, 1017–1025. <https://doi.org/10.1016/j.phytochem.2007.01.008>.
- Ponce, N., Ziegler, V.H., Stortz, C.A., Sozzi, G.O., 2010. Compositional changes in cell wall polysaccharides from japanese plum (*Prunus salicina Lindl.*) During growth and on-tree ripening. *J. Agric. Food Chem.* 58, 2562–2570 <https://10.1021/jf9039099>.
- Posé, S., Paniagua, C., Matas, A.J., Gunning, A.P., Morris, V.J., Quesada, M.A., Mercado, J.A., 2019. A nanostructural view of the cell wall disassembly process during fruit ripening and postharvest storage by atomic force microscopy. *Trends Food Sci. Technol.* 87, 47–58. <https://doi.org/10.1016/j.tifs.2018.02.011>.
- Rodriguez-Dominguez, C.M., Forner, A., Martorell, S., Choat, B., Lopez, R., Peters, J.M.R., Pfautsch, S., Mayr, S., Carins-Murphy, M.R., Mcadam, S.A.M., Richardson, F., Diaz-Espejo, A., Hernandez-Santana, V., Menezes-Silva, P.E., Torres-Ruiz, J.M., Batz, T.A., Sack, L., 2022. Leaf water potential measurements using the pressure chamber: synthetic testing of assumptions towards best practices for precision and accuracy. *Plant Cell Environ.* 45, 2037–2061. <https://doi.org/10.1111/pce.14330>.
- Rolle, L., Siret, R., Segade, S.R., Maury, C., Gerbi, V., Jourjon, F., 2012. Instrumental texture analysis parameters as markers of table-grape and winegrape quality: a review. *Am. J. Enol. Vitic.* 63, 11–28 <https://10.5344/ajev.2011.11059>.
- Saei, H., Sharifani, M.M., Dehghani, A., Seifi, E., Akbarpour, V., 2014. Description of biomechanical forces and physiological parameters of fruit cracking in pomegranate. *Sci. Hortic.* 178, 224–230. <https://doi.org/10.1016/j.scienta.2014.09.005>.
- Schumann, C., Sitzenstock, S., Erz, L., Knoche, M., 2020. Decreased deposition and increased swelling of cell walls contribute to increased cracking susceptibility of developing sweet cherry fruit. *Planta* 252, 96 <https://10.1007/s00425-020-03494-z>.
- Sensoy, S., Ertek, A., Gedik, I., Kucukyumuk, C., 2007. Irrigation frequency and amount affect yield and quality of field-grown melon (*Cucumis melo L.*). *Agric. Water Manag.* 88, 269–274. <https://doi.org/10.1016/j.agwat.2006.10.015>.
- Sirisomboon, P., Tanaka, M., Akinaga, T., Kojima, T., 2000. Evaluation of tomato textural mechanical properties. *J. Texture Stud.* 31, 665–677. <https://doi.org/10.1111/j.1745-4603.2000.tb01027.x>.
- Sirisomboon, P., Tanaka, M., Kojima, T., 2012. Evaluation of tomato textural mechanical properties. *J. Food Eng.* 111, 618–624. <https://doi.org/10.1016/j.jfoodeng.2012.03.007>.
- Tafolla-Arellano, J.C., Báez-Sañudo, R., Tiznado-Hernández, M.E., 2018. The cuticle as a key factor in the quality of horticultural crops. *Sci. Hortic.* 232, 145–152. <https://doi.org/10.1016/j.scienta.2018.01.005>.
- Verbancić, J., Lunn, J.E., Stitt, M., Persson, S., 2018. Carbon supply and the regulation of cell wall synthesis. *Mol. Plant.* 11, 75–94. <https://doi.org/10.1016/j.molp.2017.10.004>.
- Villordon, A., Gregorie, J.C., Labonte, D., 2020. Direct measurement of sweet potato surface area and volume using a low-cost 3d scanner for identification of shape features related to processing product recovery. *HortSci* 55, 722–728. <https://doi.org/10.21273/HORTSCI14964-20>.
- Wang, C., Bai, D., Li, Y., Yao, B., Feng, Y., 2021. The comparison of different irrigation methods on yield and water use efficiency of the jujube. *Agric. Water Manag.* 252, 106875 <https://doi.org/10.1016/j.agwat.2021.106875>.
- Wang, H., Chen, F., Yang, H., Chen, Y., Zhang, L., An, H., 2012. Effects of ripening stage and cultivar on physicochemical properties and pectin nanostructures of jujubes. *Carbohydr. Polym.* 89, 1180–1188. <https://doi.org/10.1016/j.carbpol.2012.03.092>.
- Wang, S., Liu, C., Su, X., Chen, L., Zhu, Z., 2023. Transcriptome analysis reveals key metabolic pathways and gene expression involving in cell wall polysaccharides-disassembly and postharvest fruit softening in custard apple (*Annona squamosa L.*). *Int. J. Biol. Macromol.* 240, 124356 <https://doi.org/10.1016/j.ijbiomac.2023.124356>.
- Winisdorffer, G., Musse, M., Quellec, S., Barbacci, A., Le Gall, S., Mariette, F., Lahaye, M., 2015. Analysis of the dynamic mechanical properties of apple tissue and relationships with the intracellular water status, gas distribution, histological properties and chemical composition. *Postharvest Biol. Technol.* 104, 1–16 <https://10.1016/j.postharvbio.2015.02.010>.
- Yakushiji, H., Sakurai, N., Morinaga, K., 2001. Changes in cell-wall polysaccharides from the mesocarp of grape berries during veraison. *Physiol. Plant.* 111, 188–195. <https://doi.org/10.1034/j.1399-3054.2001.1110209.x>.
- Yamaguchi, M., Sato, I., Ishiguro, M., 2002. Influences of epidermal cell sizes and flesh firmness on cracking susceptibility in sweet cherry (*Prunus avium L.*) Cultivars and selections. *J. Jpn. Soc. Hortic. Sci.* 71, 738–746 <https://10.2503/jjshs.71.738>.
- Yavuz, D., Seymen, M., Yavuz, N., çoklar, H., Ercan, M., 2021. Effects of water stress applied at various phenological stages on yield, quality, and water use efficiency of melon. *Agric. Water Manag.* 246, 106673 <https://doi.org/10.1016/j.agwat.2020.106673>.
- Zhang, L.Y., Huang, C.X., Zhao, Y., Zheng, C.J., Hu, C., 2023. Post-ripening and senescence behavior of atemoya (*Annona cherimola × A. squamosa*) under two typical storage temperatures. *Postharvest Biol. Technol.* 200, 112336 <https://10.1016/j.postharvbio.2023.112336>.